Iranian Int. J. Sci. ***1****(1) 2000*

Diagenetic Studies, a Key to Reveal the Timing of Oil Migration: an Example from the Tirrawarra Sandstone Reservoir, Southern Cooper Basin, Australia

Mohammad R. Rezaee[1] and Nicholas M. Lemon[2]
1- Geology Department, University of Tehran
Email: mrezaee@khayam.ut.ac.ir
2- National Centre for Petroleum Geology and Geophysics, University of Adelaide
Email: nlemon@ncpgg.adelaide.edu.au

Abstract

Commercial accumulation of petroleum requires several essential elements and processes which should occur in a certain sequence. Any departure from this sequence will be against petroleum accumulation. Therefore, the timing of oil migration and its emplacement in a reservoir is very important for petroleum geologists.

In the present work, a sequence of diagenetic events has been established for the Tirrawarra Sandstone utilizing petrographic studies, scanning electron microscopy, stable isotope, fluid inclusion microthermometry, electron microprobe analysis, cathodoluminescence observations and X-Ray diffraction.

Based on an integrated study, the timing of oil migration has been constrained with relation to other diagenetic events. Entrapment of hydrocarbon between quartz and siderite cement phases has indicated that migration of hydrocarbon has occurred at temperature range between 80°C and 102°C.

This paper discusses the diagenetic history of the Tirrawarra Sandstone reservoirs in detail and then correlates diagenetic events and the timing of hydrocarbon migration.

Keywords: *Diagenesis, hydrocarbon migration, quartz cement, siderite cement, fluid inclusion microthermometry.*

1. Introduction

The timing of hydrocarbon migration into the reservoir is one of the major studies of petroleum geologists. The goal of the present paper is to introduce a new approach for detail elaboration of oil migration into a clastic hydrocarbon reservoir in South Australia, Tirrawarra Sandstone. The Tirrawarra Sandstone is one of the major hydrocarbon reservoirs in the Cooper Basin, the largest onshore petroleum province in Australia. More than 6 TCF (170 Tm^3) gas and 300 MMSTB (48 ML) gas condensate and 2000 KL of oil have been estimated in more than 110 gas and oil fields in the Cooper Basin (Heath, 1989; Laws, 1989). The basin fill has a maximum thickness of 1300m and consists dominantly of lacustrine-fluvial deposits with local glacio-fluvial and rare paraglacial aeolian sediments.

The Tirrawarra Sandstone is composed mainly of fine- to coarse-grained sandstones with thin intercalations of siltstones, shales and coal beds. Seven facies associations are recognized in the Tirrawarra Sandstone in the Moorari and Fly Lake Fields. These facies associations are interpreted to have been deposited in seven depositional environments including braid-delta (medial & distal), back barrier marsh, beach barrier, lacustrine, meandering fluvial and aeolian environments (Rezaee, 1996).

2. Methods of study

One hundred and thirty samples from the Tirrawarra Sandstone were collected adjacent to core plugs from cores from 14 wells in the Moorari and Fly Lake Fields (Fig. 1). Detailed sedimentological descriptions of the cores were carried out, and a variety of depositional environments were sampled. The lithologies sampled were mainly sandstone, representative of different lithofacies recognized during core description. The samples were characterized using the techniques described below.

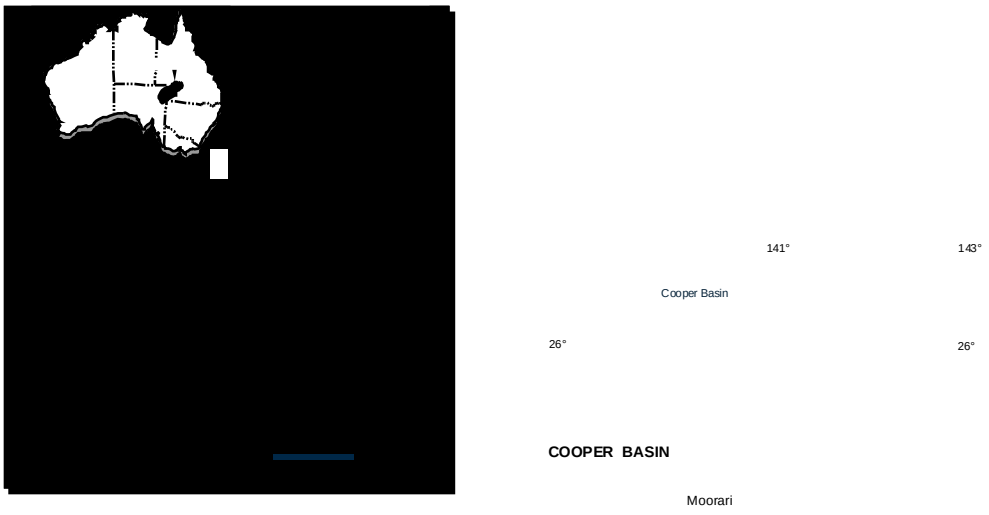

Figure 1 - Map of the Cooper Basin and the location of the Moorari and Fly Lake Fields.

2.1. Optical petrography

Thin sections were prepared for all samples, cut perpendicular to the bedding plane following impregnation of the samples with blue-dyed epoxy resin to facilitate the recognition of porosity. Quantitative estimates of sandstone mineralogy (modal composition) and porosity were determined by point-counting (400-600 counts per thin section). Approximately 100 grains were measured in each slide, using the long dimension of each grain to estimate the mean grain size and sorting of the samples.

2.2. X-ray mineralogy

Bulk-rock XRD analyses were carried out on 45 representative core samples. The samples were gently crushed in ethanol using an agate mortar and pestle, and then dried in an oven at a temperature less than 60°C to minimize clay damage. Randomly-oriented powders were prepared by pressing into a cavity-mount in an aluminium holder.

The clay fraction (< 2 μm) was separated by settling through a water column under gravity. Separated clay fractions were Mg- and glycol-saturated on ceramic plates held under vacuum.

The prepared samples were run in a *Philips PW* 1050 X-ray diffractometer at 50 kV and 35 mA, using Co Kα radiation, at a speed scan at 2°/minute. Mineral identification was checked by comparison with Joint Committee on Powder Diffraction Standards (JCPDS) files using Traces™ software.

2.3. Scanning Electron Microscopy (SEM)

SEM studies were carried out on 61 representative broken rock surfaces and polished sections coated with carbon and gold/palladium to study the texture, pore type and authigenic minerals. To obtain additional information on paragenetic relationships of the sandstone using a *Philips XL20* electron microscope connected to a back-scattered electron (BSE) detector was used. Quantitative energy dispersive X-ray (EDX) analysis was used to study the composition of representative authigenic minerals. Selected polished thin sections were examined using back-scattered electron (BSE) imaging.

2.4. Cathodoluminescence (CL) Microscopy

Sixteen samples were studied by CL to identify quartz cement stratigraphy. A *Patco ELM-RX* luminoscope was used in conjunction with a *Leitz Orthomat E automatic* camera. Electron gun voltages and beam currents of 25 kV and 200 *m*A were used whilst the polished thin sections were held under vacuums between 0.07 and 0.01 Torr. CL photomicrographs were taken at 3 to 7 minute exposure times in integral metering mode with *Kodak Ektapress* 1600 ASA film.

2.5. Electron Microprobe Analysis

The quantitative elemental compositions of quartz and siderite cements were determined on polished thin sections covered with a thin layer of carbon, using a *CAMECA SX 51* electron microprobe at 15 kV, operating with a 20 nA beam current and 0.25-0.5 *?p*m beam diameter. The back-scattered electron (BSE) imaging system linked to the electron microprobe was used to detect zonation in the siderite cement, and compositional analyses were carried out for each zone. The ZAF correction (the effect of atomic number, absorption, and

fluorescence) was used for quantitative elemental concentration. For siderite cements, results were normalized to 100 mol % Fe + Mn, Mg and Ca. The precision of analyses was ±2% for major elements. Standards used for siderite cements were: MgO for Mg; wollastonite for Ca; rhodonite for Mn; Fe_2O_3 for Fe. Chemical analyses of detrital and authigenic quartz on six samples were obtained using standards: garnet for Al, copper metal for Cu, rhodonite for Mn, galena for Pb, rutile for Ti, and garnet for Fe. At 60 seconds counting time, the detection limit for Pb was 100 ppm and 80 ppm for the other elements.

2.6. Carbon and Oxygen Isotopes

Oxygen and carbon isotope analyses were carried out on 18 core samples following selection of the samples using optical and bulk XRD methods. Only samples containing relatively high amounts of siderite cement were selected for stable isotope analysis. The samples were crushed to a fine dry powder, and then left to react with 100% phosphoric acid under vacuum at 100°C overnight (Rosenbaum & Sheppard, 1986). The resultant carbon dioxide was purified according to conventional techniques (McCrea, 1950) and analysed on a 6-inch, dual collector, *VG Micromass 602E* mass spectrometer. The acid correction factors of Rosenbaum and Sheppard (1986) were used to compensate for oxygen isotope fractionation. Stable isotope values are reported in the δ-notation in parts per thousands (‰). All oxygen isotope ratios are reported relative to standard mean ocean water (SMOW) (Craig, 1961), using the relation: $\delta^{18}O_{SMOW} = 1.03091*\delta^{18}O_{PDB} + 30.91$ (Coplen *et al.*, 1983). All carbon isotope values are reported relative to the *Bellemnitella americana* from the PeeDee Formation (PDB) (Craig, 1957).

2.7. Fluid Inclusion Microthermometry

A total of 18 samples were selected for fluid inclusion microthermometry of siderite and quartz cements. Fluid inclusion microthermometry was carried out using double-sided polished sections approximately 140 microns thick, prepared at

temperatures below 40°C. Only primary fluid inclusions, which represent minimum precipitation temperatures (Roedder, 1979; Jourdan *et al*., 1987; Walderhaug, 1990) were analyzed using a Fluid Inc. Reynolds stage and a *Leitz* optical microscope equipped with a 100× objective combined with 12.5× oculars. Reproducible microthermometry of inclusions ranging in size between 2 and 6 microns was achieved using the cycling method (Reynolds, 1978). In all of the quartz cement samples, two-phase liquid-vapor fluid inclusions were trapped close to the surface of the detrital grain and along CL boundaries within the quartz cement. In the siderite cements, the fluid inclusions were mostly equidimensional suggesting that no stretching had occurred. Because the fluid inclusions were small, it was not possible to observe the final melting of ice. The microthermometry measurement precision is ± 1°C.

3. DIAGENETIC EVENTS

According to McBride (1989), diagenesis is defined as the chemical and physical modification of sediments after deposition and prior to the onset metamorphism. Mechanical compaction, chemical compaction, cementation, dissolution, and replacement are the diagenetic processes that are responsible for modification of original intergranular porosity. Diagenetic events have resulted in reduction of porosity and permeability of the Tirrawarra Sandstone (Rezaee and Lemon, 1996). Dissolution of labile detrital grains and cement in the course of diagenesis is the only exception to this trend. Mechanical compaction and cementation are the principle factors which influence primary porosity. The effect of these two factors is controlled by composition, a facies-dependent parameter.

3.1. Compaction

Evidence of mechanical compaction in the Tirrawarra Sandstone seen in thin-section, includes plastic deformation of rock fragments, grain slippage and rearrangement and mica

bending. To evaluate the intensity of compaction quantitatively, a new equation was used in this study as "Compaction Index". The Compaction Index was defined by the following equation:

$$Compaction\ Index = \left[\frac{IGV_O - IGV}{IGV_O} \right] \times 100$$

where IGVo is the original intergranular volume at the time of deposition; and IGV is the present intergranular volume. IGVo was calculated for each sample following the method of Beard and Weyl (1973), using knowledge of sample grain size and sorting. IGV is the sum of intergranular porosity and total cement.

The Compaction Index in the Tirrawarra Sandstone varies from 3% to 95%. Since the maximum depth of burial of the samples studied does not vary significantly, the major parameters which control compaction are mineralogical composition and the occurrence of quartz cement, factors which are in turn controlled by depositional processes.

Chemical compaction can be distinguished both in thin sections and hand specimens by the presence of stylolites, concavo-convex and sutured grain contacts and pressure dissolution seams. It is common in finer-grained samples containing clay, pseudomatrix, and carbonaceous material. In these types of sandstones, the effect of carbonaceous materials and clays to promote chemical dissolution is obvious (cf. Heald, 1959; Thomson, 1959; Weyl, 1959; Füchtbauer, 1967; Houseknecht & Hathon, 1987; Ehrenberg, 1990; Bjørkum, 1996). Pressure solution in the Tirrawarra Sandstone is facies-dependent, and is most prominent in intervals that were originally low in permeability and porosity.

3.2. Cementation

Three main types of cements identified in the Tirrawarra Sandstone samples including quartz, siderite and clays. Dead oil and inclusion of hydrocarbons are trapped between different

phases of quartz and siderite cements. Obviously timing of those cement phases that oil has trapped between them can help us to identify time of hydrocarbon migration and emplacement.

3.2.1 Quartz Cements

Quartz, in the form of syntaxial rims, is the dominant cement in the Tirrawarra Sandstone and ranges from zero to 19%. Quartz cementation appears to be developed very early in some samples with low ductile rock fragment content. This is indicated by the preservation of the original intergranular volume (IGVo) (Fig. 2). Quartz overgrowths grew into the primary pores, largely filling them although the initial intergranular porosity is not completely occluded in this way.

3.2.1.1 Cathodoluminescence Microscopy of Quartz Overgrowth

Three zones of quartz cement was identified by cathodoluminescence observation of 16 Tirrawarra samples (Rezaee & Tingate, 1996; 1997). The earliest zone (dark, yellowish-brown luminescence) is here termed Z1 and occurs as overgrowths developed on detrital quartz grains. The second zone (Z2) has a bright blue luminescence that can be easily distinguished from that of the other zones. The third and latest zone (Z3) has similar CL colors to the Z1 cement. Where the second zone is absent, it is not possible to differentiate the first and the third zones.

Dead oil is trapped between Z2 and Z3 zones of quartz cement (Fig. 3).

3.2.1.2 Electron Microprobe Analyses of Quartz Overgrowth

To identify cathodoluminescence color variations, concentration of Fe, Ti, Mn, Al, Cu and Pb elements was assessed for different zones of quartz cement by electron microprobe analyses. These elements are associated with enhanced quartz cathodoluminescence (Sprunt, 1981; Matter & Ramseyer, 1985). Except for aluminium, the rest of the elements do not

show meaningful variation between cement zones. The average aluminium concentration is 237, 538 and 58 ppm for Z1, Z2 and Z3 quartz cements (Table 1). The bright blue color of the Z2 quartz cement appears to be related to its high aluminium content, which is possibly associated with accompanying charge balancing cations (Ramseyer & Mullis, 1990; Perny *et al.*, 1992). Electron microprobe analysis was also carried out on several detrital grains in the Tirrawarra Sandstone which have an average aluminium concentration of 35 ppm (Table 1).

3.2.1.3 Quartz Overgrowth Fluid-inclusion Homogenization Temperatures

Fluid-inclusion microthermometry was accomplished using primary fluid-inclusions trapped within each cement zone. Homogenization temperatures of fluid-inclusions within different zones of quartz cement indicate that quartz cement precipitated at temperatures between 65 and 130°C, unless the fluid-inclusions re-equilibrated during burial (cf. Osborne & Haszeldine, 1993; Haszeldine & Osborne, 1993). However, the consistent differences in homogenization temperatures between different zones of quartz cement indicate that the fluid-inclusions have not re-equilibrated (Fig. 4). Low-temperature fluid-inclusions (65 - 80°C) occur in Z1 quartz cement which is well developed in samples with a quartzarenite composition and high intergranular volume (IGV). Primary fluid-inclusions within Z2 cement have a homogenization temperature range of 80 to 100°C. Homogenization temperatures of most fluid-inclusions within Z3 cement were approximately 130°C, indicating the minimum precipitation temperature of the late stages of quartz cement.

Figure2 - SEM view of a medium grained, quartz-rich, well-cemented sandstone with dominant primary intergranular porosity. Note the excellent connectivity between pore spaces. Sample M3-9405, Moorari-3, 2821.5 m. Scale bar = 100 ?gn.

Figure 3 - Early generated hydrocarbons have been trapped prior to the latest zones of quartz cement. In this example it can be seen that a relatively thin zone of quartz overgrowth (arrow) is separated by dead oil from earlier quartz cements. Sample M3-9415, Moorari-3, 2824.5 m.

Table 1 - Mean values of trace elements for different zones of quartz cement and detrital quartz grains.

	Z1 (ppm)	Z2 (ppm)	Z3 (ppm)	Grain (ppm)
Al_2O_3	237	538	58	35
FeO	74	119	206	39
TiO_2	75	24	112	84
MnO	113	104	146	60
CuO	125	191	76	52
PbO	251	70	276	149

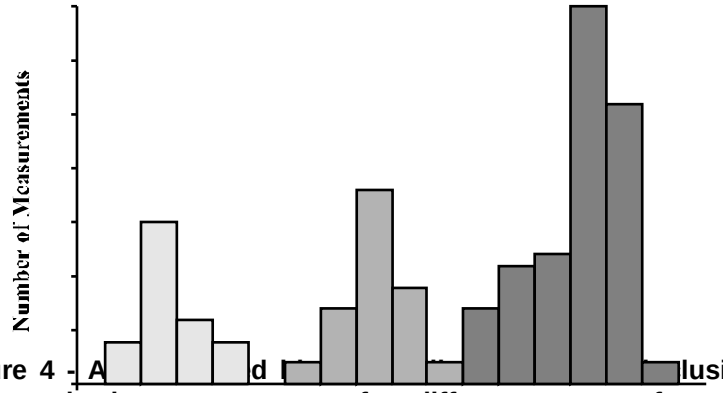

Figure 4 - A[illegible]d [illegible]lusion homogenization temperatures for different zones of quartz cement. (Z1 = innermost zone, Z2 = middle zone and Z3 = outermost zone of quartz cement).

3.2.2 Siderite cements

Siderite cement occurs in varying proportions in the Tirrawarra Sandstone, and constitutes up to about 30% of rock volume in some. Under the petrographic microscope and SEM, the siderite habit is generally micritic, isolated, or a pore-filling cement. Under the SEM and electron microprobe and using BSE imaging techniques, three main generations of siderite cement were identified, including an early (S1), middle (S2), and late generation cement (S3) (Fig. 5).

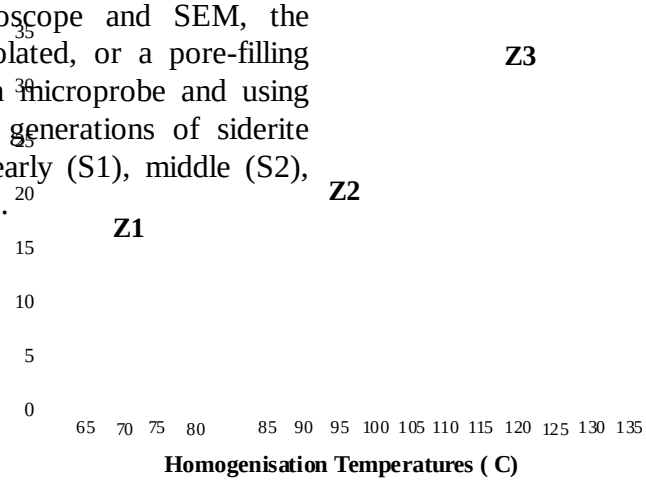

Figure 5 - BSE image showing different stages of siderite cement. S1 displays a white color whilst the surrounding S2 (medium grey) is characterized by a variable internal composition and complex zoning. S3 is a relatively homogeneous, late-generation pore-filling cement. Note the irregular dissolution boundary between S1 and S2, and between S2 and S3 (arrows). Sample M1-9598, Moorari-1, 2925.5 m. Scale bar = 50 ?m.

Under the optical microscope, S1 has a blotchy appearance, displays a moderately light to dark brown color and appears devoid of fluid-inclusions. In BSE image, S1 is light-coloured and appears homogenous. Electron microprobe analysis for S1 shows a high Fe/Mg ratio. The S1 elemental composition ranges from $(Fe_{97.7\%}Mg_{0.8\%}Ca_{0.7\%}Mn_{0.8\%})CO_3$ to $(Fe_{93.4\%}Mg_{2\%}Ca_{3.3\%}Mn_{1.3\%})CO_3$, with the average composition being $(Fe_{96\%}Mg_{1\%}Ca_{1.7\%}Mn_{1.3\%})CO_3$ (Table 2). In samples which are dominated by S1 (92-98%), oxygen isotope compositions range from +14.1‰ to +15.1‰, with $\delta^{13}C$ compositions varying between -3.8 and +1.45‰ (Table 3).

Table 2 - Average elemental composition (mole%) of different stages of siderite cement generations (S1, S2, S3) acquired by microprobe analysis.

	S1	S2	S3
FeO (%)	95.7	83.0	76.8
MgO (%)	1.0	14.3	21.8
CaO (%)	1.9	0.8	0.3
MnO (%)	1.4	1.8	1.1

Petrographically, S2 is mostly in the form of colorless rhombs which enclose S1. In BSE images, S2 displays distinct irregular compositional zoning and minor dissolution indicating pore fluid chemistry fluctuations occurred during cementation. Electron microprobe analyses reveal different elemental compositions and variable substitution of Mg for each of the S2 sub-generations. S2 compositions range from $(Fe_{87.2\%}Mg_{9.5\%}Ca_{0.7\%}Mn_{2.6\%})CO_3$ to $(Fe_{56.7\%}Mg_{42.2\%}Ca_{0.15\%}Mn_{0.95\%})CO_3$, with the average composition being $(Fe_{74\%}Mg_{24\%}Ca_{0.8\%}Mn_{1.2\%})CO_3$ (Table 2) representing sideroplesite for the light-colored zone and pistomsite for the medium to dark-colored zone (classification of Deer *et al.*, 1992). In samples in which S2 is the dominant carbonate cement phase (93-98%), oxygen isotope values range from +12.3‰ to +12.8‰, and carbon isotope values between -9.2‰ and -7.9‰. The mean $\delta^{13}C$ composition is about -8.6‰, and the average $\delta^{18}O$ composition is +12‰ for S2 (Table 3).

Under the optical microscope, S3 is blocky, colorless, very clear cement, postdating S1 and S2. BSE images show that S3 is a relatively homogenous cement generation (when compared to S2), characterized by an initial high Mg content (pistomsite) grading into a relatively thick, homogenous sideroplesite cement. Electron microprobe analyses indicate extensive substitution of Mg, with an average composition of $(Fe_{75.5\%}Mg_{23\%}Ca_{0.5\%}Mn_{1\%})CO_3$ for S3 (Table 2). In samples which contain the highest proportion of S3 (95-97%), oxygen isotope

compositions range from +6.1‰ to +6.6‰, with $\delta^{13}C$ compositions varying between -11.1‰ and -10.4‰. For these samples, mean oxygen and carbon isotope values are about +6‰ and -11‰ respectively (Table 3).

Dead oil and hydrocarbon fluid inclusions are trapped between S2 and S3 stages of siderite cement.

Table 3 - Carbon and oxygen isotope data of the Tirrawarra Sandstone siderite cements.

Sample	?13C (PDB‰)	?18Omeas (PDB‰)	?18Omeas (SMOW‰)	S1(%)	S2(%)	S3(%)
M5-9583	-10.37	-23.38	6.6	0	3	97
M2-10145	-11.13	-23.83	6.15	0	5	95
M4-9574	-10.68	-21.39	8.59	0	40	60
M7-9606	-10.49	-22.70	7.28	15	30	55
M2-10116	-8.13	-19.12	10.86	10	43	47
F1-9417	-3.83	-15.80	14.18	19	38	43
M6-9737	-9.70	-18.79	11.19	8	51	41
F1-9431	-4.22	-18.50	11.48	0	60	40
M1-9598	-7.07	-17.56	12.42	36	38	26
M3-9440	-5.98	-15.37	14.61	80	13	7
F2-9583	1.45	-15.84	14.14	92	3	5
M3-9503	-7.97	-17.67	12.31	0	98	2
M1-9613	-9.22	-18.23	11.75	3	95	2
M4-9554	-8.95	-17.17	12.81	5	93	2
M9-9732	-4.99	-15.71	14.27	60	39	1
M3-9422	-3.87	-14.85	15.13	98	1	1
M1-9620	-6.23	-16.70	13.28	15	85	0
F4-9441	1.46	-16.01	13.97	100	0	0

3.2.2.1. Siderite Cement Fluid-inclusion Analysis

S1 siderite cement is devoid of fluid-inclusions while S2 and S3 siderite cements have equidimensional fluid-inclusions. Homogenization temperatures of S2 fluid-inclusions range from 66 to 76°C, with a median around 68°C (Fig. 6). Fluid-inclusion results for S3 indicate an homogenization temperature of between 98 and 114°C, with a median about 102°C (Fig. 6).

Compositional zoning is evident in the S2 siderite cement indicating that the cements precipitated from solution and did not undergo recrystallisation during burial diagenesis. No unstable precursor for siderite is known, and there exists no

documented case of siderite recrystallisation (Mozley & Carothers, 1992). For these reasons, fluid-inclusions are thought to provide a genuine record of the temperatures at which the siderites in the Tirrawarra Sandstone crystallized, unless resetting of the inclusions (Prezbindowski & Larese, 1987; McLimans, 1987; Prezbindowski & Tapp, 1991) occurred. However, consistent differences in homogenization temperatures between S2 and S3 (Fig. 6) suggest the fluid-inclusions did not undergo re-equilibration in view of the fact that appreciable differences in the size of the fluid-inclusions were not detected between S2 and S3.

No fluid-inclusion data are available for S1, but the cement stratigraphy would suggest that S1 crystallized at temperatures lower than those for S2, ie. less than about 66°C.

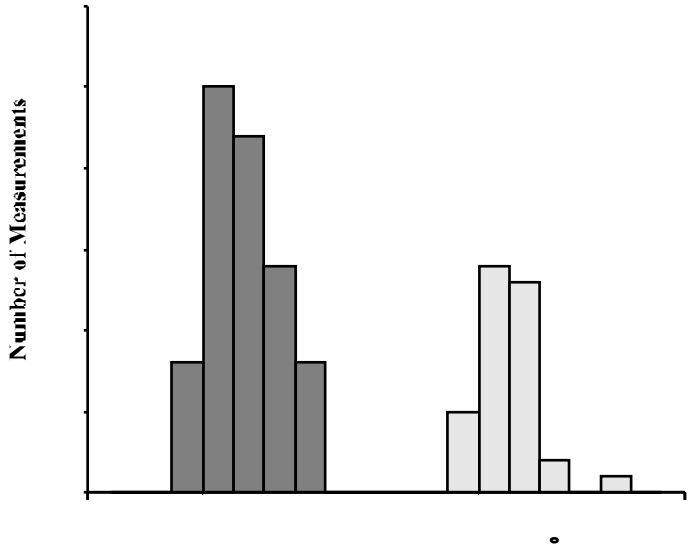

Figure 6 - Fluid inclusion homogenization temperatures for the middle (S2) and late generations (S3) of the Tirrawarra Sandstone siderites.

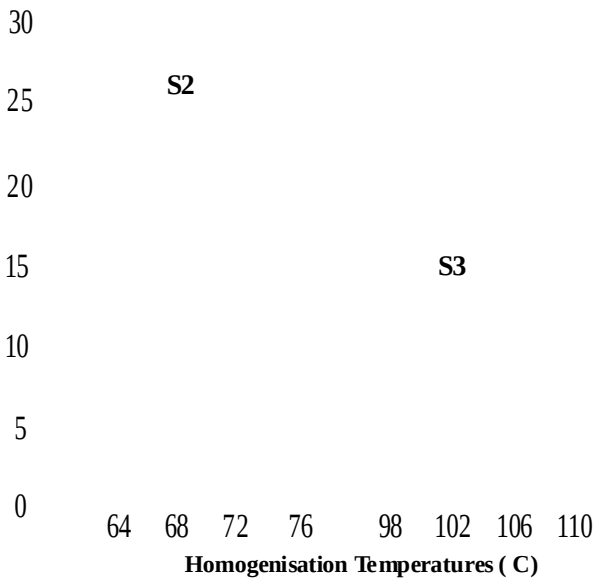

3.2.3. Clay Cements

SEM, EDX, and XRD analyses of the clay fraction (<2 ?m size) indicate that the clays are dominated by kaolinite and illite. Under the optical microscope and SEM, kaolinite occurs as euhedral booklets which infill pore spaces and are intergrown with quartz overgrowths. Kaolinite in the form of pseudo-hexagonal stacked plates is pervasive in nearly all of the Tirrawarra Sandstone samples (Fig. 7).

Figure 7 - SEM view of pore-filling, euhedral kaolinite booklets. Note the abundant microporosity associated with kaolinite booklets. Sample M3-9405, Moorari-3, 2821.5 m. Scale bar = 50 ?m.

Genetically, there are two types of authigenic kaolinite in the Tirrawarra Sandstone. The first type is formed by the complete replacement of an original or precursor grain. This kind of kaolinite shows the exact margin of the original grains. The second type is precipitated directly from pore fluids. This pore-filling cement alters the intergranular macroporosity to microporosity, which exists among the kaolinite booklets. This type of kaolinite, which is coarser-grained than the first type

(about 40 microns), is often vermicular, shows less packing, and is also intergrown with the quartz cement.

Illite is the next most important clay mineral in most of the samples. Its authigenic nature is evident from its fibrous, lath- or lettuce-like habit. The mineral is thought to have largely formed as a replacement product of chemically unstable rock fragments. In some rare instances illite occurs as pore bridging cement.

4. DISCUSSION

4.1. Quartz Cement

Quartz cement in siliciclastic sequences is commonly a major diagenetic phase that affects hydrocarbon reservoir quality. In most sedimentary basins, it forms at temperatures between 60 and 145°C (Walderhaug, 1994) and many sources of silica have been proposed. McBride (1989) reviewed over 20 silica sources for quartz cement proposed by various workers in numerous basins. The most likely sources of silica for quartz cement in the Tirrawarra Sandstone were discussed in detail by Rezaee and Tingate (1997) and are discussed briefly here.

Dissolution of feldspar is reported as a silica source for quartz cement (Fothergill, 1955; Siever, 1957; Hawkins, 1978; Morad & Aldahan, 1987). During feldspar dissolution, kaolin forms and silica is released according to the reaction:

$$2H_2CO_3 + H_2O + 2KAlSi_3O_8 \text{ ?‡ } Al_2Si_2O_5(OH)_4 + 4SiO_{2(aq.)} + 2K^+ + 2HCO_3^-$$

In this reaction, $1cm^3$ of K-feldspar yields 0.43 cm^3 of quartz and 0.46 cm^3 of kaolinite. In the Tirrawarra Sandstone, apart from a few heavily-altered feldspar grains, the great majority of samples contain no feldspar. Prismatic kaolinite pseudomorphs and oversize pores suggest that feldspar was an important detrital component at deposition. Williams *et al*. (1985) has also suggested that feldspathic acid igneous rocks were a major sediment source for the Tirrawarra Sandstone. The absence of feldspar and the abundance of authigenic kaolinite suggests that

the kaolinite was derived from feldspar alteration. Assuming all kaolinite in the Tirrawarra Sandstone samples was derived from feldspar alteration, mass balance calculations indicate that the silica generated would have been sufficient to produce 61 percent of the total observed quartz cement.

Pressure solution of quartz grains at grain contacts can be an important source of silica (Waldschmidt, 1941; Heald, 1955; Füchtbauer, 1974; Sibley & Blatt, 1976; Bjørlyyke *et al*., 1986; Houseknecht, 1988; Dutton & Diggs, 1990; Bjørlyyke & Egeberg, 1993; Dutton, 1993; Walderhaug, 1994; Oelkers *et al*., 1996). Pressure solution is more extensive in finer-grained sandstones than in coarse-grained sandstones (Stephan, 1970; Pittman, 1979; Houseknecht, 1984; Bjørlykke *et al*., 1986; Porter & James, 1986; Houseknecht & Hathon, 1987; and Bjørlykke & Egeberg, 1993). Chemical compaction in the form of intergranular pressure solution and stylolites is very common in the Tirrawarra Sandstone. This feature is significant in finer-grained sandstones and sandstones rich in rock fragments and is considered to be an important source of silica for quartz cement in the Tirrawarra Sandstone.

Replacement of quartz grains by carbonate minerals has been reported by many authors (e.g., Walker, 1960; Burley & Kantorowicz, 1986). In the Tirrawarra Sandstone, quartz overgrowths and quartz grains are embayed by siderite cement. This replacement, however, is not very common and this process cannot be considered an important source for silica.

Aluminium analyses of different zones of quartz cement show that large differences in aluminium content. It is more likely that total aluminium concentrations have fluctuated over the diagenetic history of the Tirrawarra Sandstone. The formation has experienced discrete episodes of feldspar dissolution and kaolinite precipitation which were probably associated with pore fluids of higher aluminium content. Contemporaneous Z1 and Z2 quartz cements have a high aluminium content,

reflecting an elevated aluminium content in the pore fluid. Z3 cement, in contrast, formed later, without this contemporaneous aluminium source. The high Al content of Z2 quartz cement and its homogenization temperature agrees with the influence of organic acid generated during kerogen maturation and hydrocarbon expulsion on the formation of this zone of quartz cement (Rezaee and Tingate, 1997). This is supported by entrapment of dead oil between Z2 and Z3 quartz cements.

Various thermal scenarios were modeled using vitrinite data in order to constrain the timing of the quartz cements in the Tirrawarra Sandstone using *BasinMod*?-. Measured vitrinite reflectance values and values calculated from the methylphananthrene index (MPI) using oil in the Tirrawarra Sandstone within the Fly Lake and Moorari Fields are both close to 1.0 (Tupper and Burckhardt, 1990), suggesting that migration was local or both reservoir and oil have been affected by post-emplacement burial. In a simple thermal model with a constant (present) heatflow without erosion at unconformities, the dominant feature in the thermal history is Cretaceous burial. This causes rapid heating of the Tirrawarra Sandstone and forces it into the oil window (Fig. 8). Model vitrinite values are close to those measured at the level of the Tirrawarra Sandstone. However, measured vitrinite values from higher up the studied wells are significantly less than the calculated values. This is likely to be related to a recent increase in geothermal gradients and localized aquifer-related heating, noted in other parts of the Cooper/Eromanga Basins (Gleadow *et al.*, 1988). If a recent increase in geothermal gradients has occurred, then the similarity between calculated and measured vitrinite values in the Tirrawarra Sandstone is fortuitous and the measured vitrinite values reflect earlier rather than present thermal conditions. Figure 8 shows a schematic time-temperature path for the Tirrawarra Sandstone based upon thermal modelling. In this history, the likely time ranges for the formation of the different phases of quartz and siderite cements are illustrated.

Based on the precipitation temperature of middle generation of siderite cement (S2), which is about 68°C, and also evidences of compositional zoning and dissolution phases related to tectonic activities about 200 Ma, erosion of about 550 meters considered to have occurred during the late Triassic in the studied area (Rezaee *et al.*, 1997). If 550 meters erosion is considered as the maximum erosion in the studied area, Z1 has been formed at approximately 200 Ma and Z2 quartz cement could have been formed at approximately 100 Ma, while Z3 quartz cement is considered to accompany or postdate oil migration into the Tirrawarra Sandstone and is believed to have formed between 100 Ma and present.

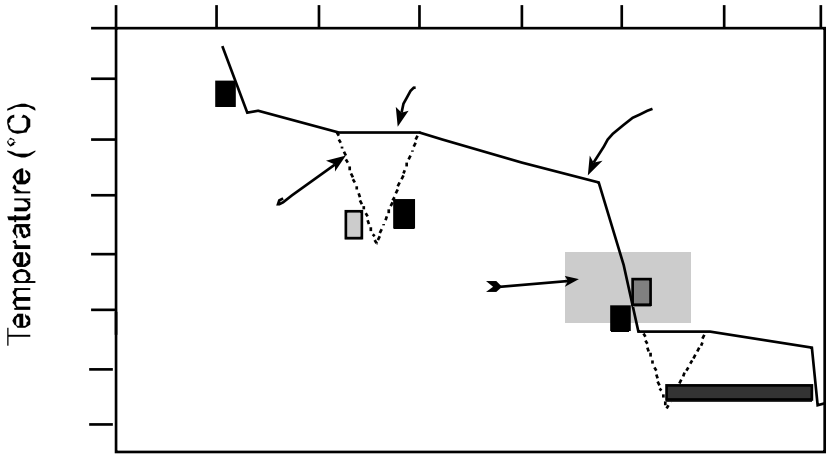

Figure 8 - Schematic thermal history of the Tirrawarra Sandstone, Fly Lake field. Time and temperature of formation of different phases of siderite and quartz cements. The time and temperature of oil migration for Tirrawarra Sandstone is shown on the figure.

It can be concluded that the first zone of quartz cement (Z1), formed at about 65°C, is derived from early dissolution of feldspar grains by acidic meteoric water flushing during late

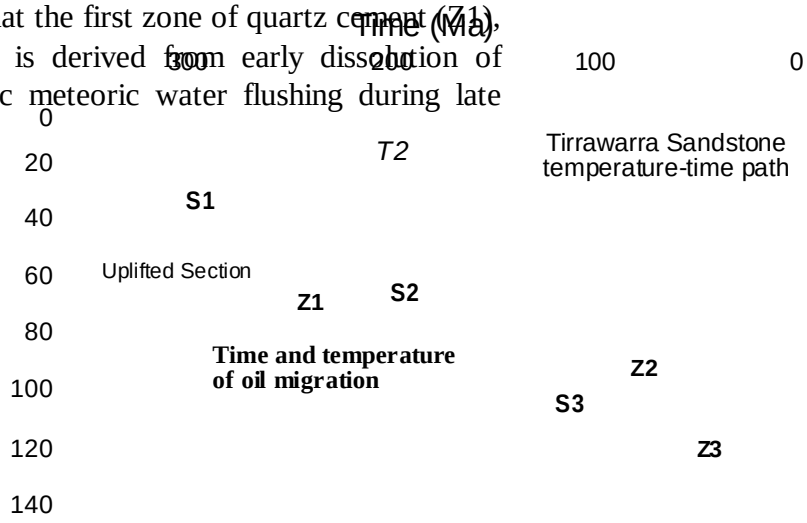

Triassic tectonic activity. The second zone of quartz cement (Z2), formed at about 100°C, originated from late dissolution of feldspar grains by organic acids generated during kerogen maturation. The third zone of quartz cement (Z3), precipitated after oil migration at about 130°C, originated mostly from stylolitization and pressure dissolution of quartz grains.

4.2. Siderite cement

The only carbonate cement present in the Tirrawarra Sandstone is siderite. Application of the back-scattered electron image analysis technique, together with bulk-rock isotope and fluid inclusion studies, has led to the identification of three main generations of siderite cement (Rezaee & Schulz-Rohjan, 1998). The first and second siderite cement generations were each followed by at least one dissolution event related to the tectonic episodes in the study area (Rezaee *et al*., 1997). The first generation of siderite (S1) is an homogeneous Fe-rich siderite with a $\delta^{13}C$ signature of +1.45‰, which probably formed during low-temperature methanogenesis (≤ 30°C) (Rezaee & Schulz-Rohjan, 1998). The second generation of siderite cement (S2) is an Mg-rich, inhomogeneous siderite characterized by complex zoning, with a $\delta^{13}C$ signature of -8.5‰. This siderite cement is thought to have formed mainly in association with the decarboxylation of organic matter at temperatures between 64 and 76°C. The third and final siderite precipitation event (S3) produced an Mg-rich, evenly banded, pore-filling siderite with average $\delta^{13}C$ of -11‰. This siderite is also interpreted to have formed during kerogen maturation, albeit at more elevated temperatures (98-110°C). It seems that organic processes associated with hydrocarbon generation and migration, controlled siderite cementation over a range of different burial conditions in the study area.

Integrating video-imaging and image analysis software, Rezaee & Schulz-Rohjan (1998) provided an efficient means of quantifying the different siderite cement generations seen under

the BSE. They introduced a new method which enabled the determination of end-member $\delta^{18}O$ and $\delta^{13}C$ compositions of individual cement generations in cases where pure, or nearly pure samples of end-member carbonate cement generations are not available for isotope analysis. Since the method can be semi-automated, the technique provided a potentially powerful tool for improved bulk-rock isotope interpretations in clastics containing multi-generation carbonate cements.

4.3. Clay Minerals

The authigenic origin of the kaolinite in the Tirrawarra Sandstone is supported by its euhedral habit. Kaolinite is stable at pH between 5 to 8 and forms at low to moderate temperatures (May *et al*., 1979; Hurst, 1980). Early authigenic kaolinite forms in meteoric pore waters with low pH and low ionic concentrations at the expense of feldspars and micas (Sommer, 1978; Bjørlykke & Brendsdal, 1986; Bjørlykke, 1988; Glasmann *et al*., 1989). In a large number of samples, the occurrence of kaolinite is associated with the original grains, identified by the original margin. The most likely precursors are believed to be feldspar grains, now completely absent in most of the Tirrawarra Sandstone samples. CL observation by Schulz-Rojahn (1991) also indicated partial and complete replacement of feldspar grains by kaolinite in the Cooper Basin. The replacement of micas by kaolinite also can be seen in a few samples although this type of kaolinitisation is not pervasive.

According to Curtis (1983), late kaolinite can be formed from Al-bearing acidic pore waters, derived mainly from maturing kerogen, in which the pH has been increased by dissolution of carbonate materials. Increasing pH causes supersaturation of the fluid which finally leads to kaolinite precipitation. In the Tirrawarra Sandstone, some of the kaolinite is formed after dissolution of the middle or late generation of siderite cement suggesting that it formed late. In the Tirrawarra Sandstone kaolinite formed during two stages. The first stage formed

relatively early, at temperatures around 60°C, when acidic meteoric water invaded the reservoir and led to dissolution of feldspar grains. The second generation of kaolinite formed during late dissolution of feldspar grains by organic acids during kerogen maturation, before hydrocarbon expulsion at temperatures around 80°C.

The crystal habit of illite in the Tirrawarra Sandstone is related to its authigenic origin. The formation of illite in the Tirrawarra Sandstone is related mainly to alteration of the labile component of rock fragments, possibly during relatively late diagenesis. In some rare instances under SEM, fine illite fibers are formed close to kaolinite booklets. This may suggest that illitization of kaolinite has occurred in the Tirrawarra Sandstone. Illitization of kaolinite is thought by Bjørlykke (1984, 1992) and by Bjørlykke *et al*., (1986) to take place at temperatures of 130 - 150°C in a closed system in presence of K-feldspar to act as the source of potassium. Bjørkum and Gjelsvik (1988) indicated that illitization of kaolinite in the presence of K-feldspar may take place at temperatures as low as 50°C, depending to the silica activity in the formation water. In the Tirrawarra Sandstone, illitization of both early and late kaolinite suggests that this process has taken place at high temperature after late feldspar dissolution by organic acids generated from decarboxylation. Dating of illite cement has supported this suggestion (Cubbit, 1999, personal communication).

4.5. Diagenetic Sequence

A combination of petrographic, stable isotope, fluid-inclusion, SEM, CL, Electron microprobe, XRD and image analysis studies were employed to construct diagenetic sequences for the studied samples. The time of hydrocarbon migration is linked to the diagenetic events.

The diagenetic sequence established during the present study (Fig. 9), in approximate chronological order, is as follows:

1. Mechanical compaction, which started soon after the deposition of the sediments;
2. Precipitation of an early generation of siderite cement (S1) at about 30°C;
3. A first phase of siderite dissolution (D1), at a temperature between 30° and 65°C, influenced by flushing with acidic meteoric waters;
4. Early dissolution of feldspar grains associated with flushing by acidic meteoric water;
5. Generation of early kaolinite, also during meteoric flushing;
6. Formation of early quartz cement (Z1) at a temperatures around 65°C;
7. Precipitation of a second generation of siderite (S2) at a temperatures of around 68°C;
8. Formation of late kaolinite during late dissolution of feldspar grains by organic acids generated during kerogen maturation;
9. A second dissolution phase of siderite (D2) at temperatures of between 68° and 102°C, by organic acids generated during kerogen maturation;
10. Formation of a second stage of quartz cement (Z2) at temperatures of between 80° and 100°C;
11. ***Hydrocarbon migration at temperatures of between 80?Y and 102?C;***
12. Precipitation of a late generation of siderite cement (S3) at temperatures about 102°C;
13. Illitization of labile components of rock fragments;
14. Chemical compaction by stylolitisation and intergranular pressure solution;
15. Formation of late quartz cement derived from pressure solution at temperatures of between 100 and 130°C.

There is a degree of overlap between diagenetic events.

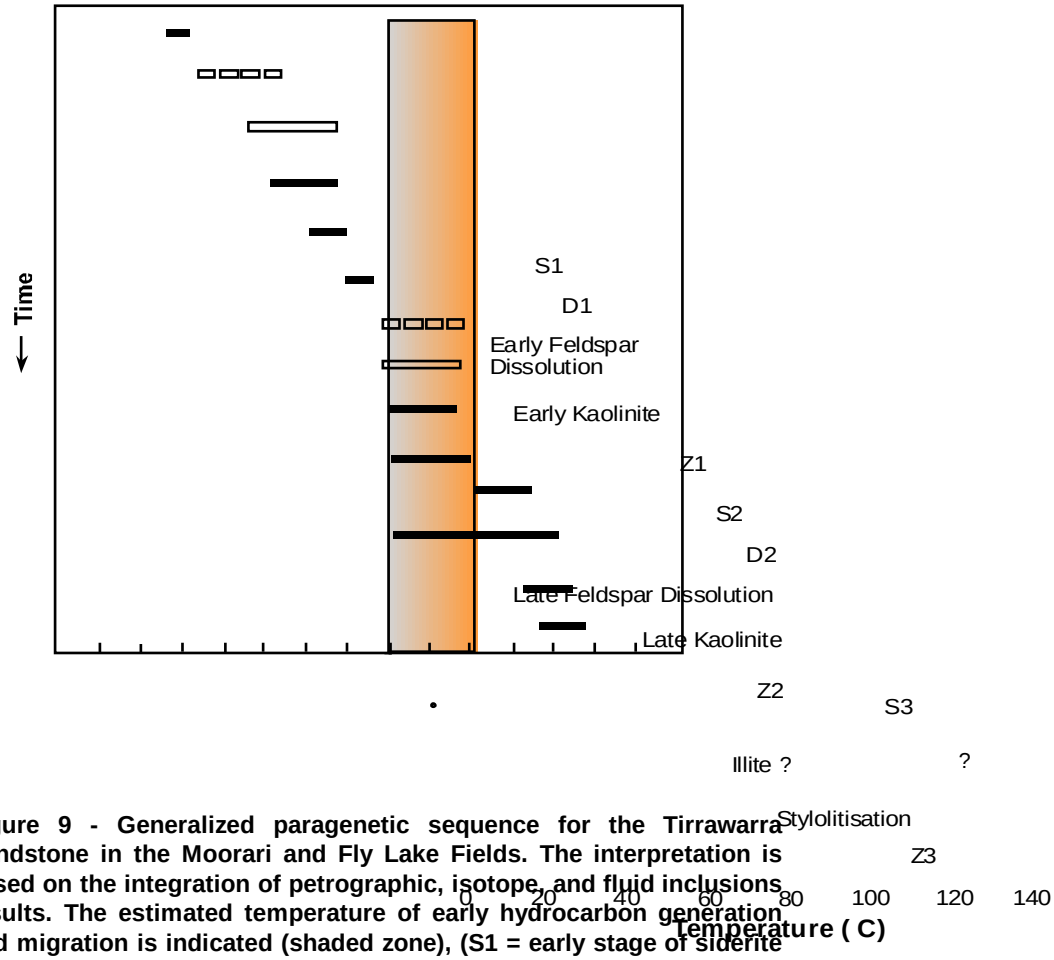

Figure 9 - Generalized paragenetic sequence for the Tirrawarra Sandstone in the Moorari and Fly Lake Fields. The interpretation is based on the integration of petrographic, isotope, and fluid inclusions results. The estimated temperature of early hydrocarbon generation and migration is indicated (shaded zone), (S1 = early stage of siderite cement; S2 = middle stage of siderite cement; S3 = late stage of siderite cement; Z1 = early quartz cement; Z2 = middle quartz cement; Z3 = late quartz cement; D1 and D2 = first and second phase of siderite dissolution respectively).

4.6. Oil Migration

There is a close relationship between the two phases of siderite dissolution and quartz cement precipitation. The early generation of siderite cement (S1) dissolved at temperatures above 30°C and below 68°C, probably due to low-pH meteoric

water interaction during which early dissolution of feldspar grains occurred. The second siderite dissolution phase, which acted on the middle generation of siderite cement (S2), occurred at temperatures between 68°C and 102°C, probably related to acidic fluids generated from kerogen maturation. Z1 and Z2 quartz cement precipitation coincided with the dissolution phases of siderite cement. Z1 formed during meteoric water flushing that led to silica release from early feldspar dissolution and also led to S1 dissolution. Z2 quartz cement precipitated during kerogen maturation, when fluid generated led to dissolution of feldspar grains and S2 siderite. Both S2 and S3 siderite and Z1 and Z2 quartz cements have bitumen trapped between them. In some samples, dead oil concentrates in the boundary zone between S2 and S3, indicating that hydrocarbon migration occurred synchronous with, or after the dissolution event but prior to S3 precipitation**.** This phenomenon has also occurred for the quartz cement and it can be seen that bitumen is trapped between quartz cement zones especially between the earlier and latest (Z3) zones. Entrapment of hydrocarbon in only quartz cement, indicates early migration of hydrocarbon between 80°C and 130°C. But the occurrence of hydrocarbon between S2 and S3 indicates narrower temperature range between 80°C and 102°C for hydrocarbon migration (Fig. 9).

This relationship also suggests that the late stage of quartz cement (Z3) formed after an early oil migration event and was followed by the main oil charge which can be seen as oil droplets snapped off in pore spaces. Quartz cementation after hydrocarbon emplacement is also reported by several workers in other basins (Walderhaug, 1990; Bjørlyyke and Egeberg, 1993; Walderhaug, 1994).

7. CONCLUSIONS

Based on the integration of data derived from different techniques, a detailed sequence of diagenetic events was

established for the Tirrawarra Sandstone in the studied area. The combination of petrography, fluid-inclusion studies, electron microprobe and cathodoluminescence examinations in the Tirrawarra Sandstone gave an indication of the timing of different phases of silica and siderite cements.

Hydrocarbon generation and migration has influenced some diagenetic effects on both rock components and cements. This includes late feldspar dissolution, S2 dissolution, late kaolinite precipitation and Z2 precipitation. Entrapment of hydrocarbon in different phases of siderite and quartz cements indicated that migration of hydrocarbon occurred at the temperature range between 80°C and 102°C.

This study shows that detailed study of paragenetic sequences and their relation to hydrocarbon generation and migration can be a valuable tool for the timing of oil migration into the reservoir.

ACKNOWLEDGMENTS

The authors gratefully acknowledge support by University of Tehran, NCPGG and SANTOS Ltd. They also wish to acknowledge SANTOS Ltd. (operator on behalf of the Cooper Basin consortium) for permission to publish this work. The manuscript was greatly improved by constructive comments from Iranian International Journal of Science reviewers.

References

Beard, D.C., and Weyl, P.K., (1973) *Influence of texture on porosity and permeability of unconsolidated sand,* AAPG Bulletin, **57**, 349-369.

Bjørkum, P.A., (1996) *How important is pressure in causing dissolution of quartz in sandstones*? Journal of Sedimentary Research, **66**, 147-154.

Bjørkum, P.A., and Gjelsvik, N., (1988) *An isochemical model for formation of authigenic kaolinite, K-feldspar and illite*

in sediments, Journal of Sedimentary Petrology, **58**, 506-511.

Bjørlykke, K., (1984) *Formation of secondary porosity: how important is it*? AAPG Memoir **37**, 217-224.

Bjørlykke, K., (1988) *Sandstone diagenesis in relation to preservation, destruction and creation of porosity*. in: G.V.,Chilingarian, and K.H., Wolf, (eds.), Diagenesis, 2. *Developments in Sedimentology*, 41. Elsevier Scientific Publications, Amsterdam, 555-588.

Bjørlykke, K., Aagaard, P., Dypvik, H., Hastings, A.S., and Harper, D.S., (1986) *Diagenesis and reservoir properties of Jurassic sandstones from the Haltenbanken area, offshore mid-Norway*, in: Habitat of hydrocarbons on the Norwegian Continental Shelf: London, Graham and Trotman Ltd., (eds. Spencer, A.M., Holter, E., Campell, C.J., Hanslien, P.H.H., Nysaether, E., Ormaasen, 275-276.

Bjørlykke, K., and Brendsdal, A., (1986) *Diagenesis of the Brent Sandstone in the Statfjord Field*, SEPM Special Publication, **38**, 157-167.

Bjørlykke, K., and Egeberg, P.K., (1993. *Quartz cementation in sedimentary basins*, AAPG Bulletin, **77**, 1538-1548.

Burley, S.D., and Kantorowicz, J.D., (1986) *Thin section and SEM textural criteria for the recognition of cement-dissolution porosity in sandstones*, Sedimentology, **33**, 587-604.

Coplen, T.B., Kendall, C., and Hopple, J., (1983) *Comparison of stable isotope reference samples*, Nature, **302**, 236-238.

Craig, H., (1957) *Isotope standards for carbon and oxygen and correction factors for mass spectrometric analysis of carbon dioxide*, Geochimica et Cosmochimica Acta, **12**, 133-149.

Craig, H., (1961) *Standards for reporting concentrations of deuterium and oxygen-18 in natural waters*, Science, 133, 1833-1834.

Curtis, C.D., (1983) *Link between aluminum mobility and destruction of porosity*, AAPG Bulletin, **63**, 380-384.

Deer, W.A., Howie, R.A., and Zussman, J., (1992) *An introduction to the rock-forming minerals*, Longman Group Limited, London, 695pp.

Dutton, S.P., (1993) *Influence of provenance and burial history on diagenesis of Lower Cretaceous Frontier Formation sandstones, Green River Basin, Wyoming*, Journal of Sedimentary Petrology, **63**, 665-667.

Dutton, S.P., and Diggs, T.N., (1990) *History of quartz cementation in the Lower Cretaceous Travis Peak Formation, East Texas*, Journal of Sedimentary Petrology, **60**, 191-202.

Ehrenberg, S.N., (1990) *Relationship between diagenesis and reservoir quality in sandstones of the Garn Formation, Haltenbanken, Mid-Norwegian continental shelf*, AAPG Bulletin, **74**, 1538-1558.

Fothergill, C.A., (1955) *The cementation of oil reservoir sands and its origin*, Proc. 4th World Petroleum Conference, Rome, 1955, 301-314.

Füchtbauer, H., (1967) *Influence of different types of diagenesis on sandstone porosity*, Proc. 7th World Petroleum Congress, **2**, 353-369.

Füchtbauer, H., (1974) *Sediments and Sedimentary rocks*, New York, N.Y., Wiley, 464p.

Glasmann, J.R., Clark, R.A., Larter, S., Briedis, N.A., and Lundegard, P., (1989) *Diagenesis and hydrocarbon accumulation, Brent Sandstone (Jurassic), Bergen High area, North Sea*, AAPG Bulletin, **73**, 1341-1360.

Gleadow, A.J.W., Duddy, I.R., Green, P.F., and Lovering, J.F., (1988) *Assessment of hydrocarbon resource potential in Australian sedimentary basins: development of fission track technique,:* End of Grant Technical Report, National Energy Research and Development and Demonstration Cooperation Project 720, 116

Haszeldine, R.S., and Osborne, M., (1993) *Fluid inclusion temperatures in diagenetic quartz reset by burial:*

implications for oil field cementation. In :Diagenesis and Basin Development (eds. Horbury, A.D., and Robinson, A.G.), American Association of Petroleum Geologists Studies in Geology, **36**, 35-46.

Hawkins, P.J., (1978) *Relationship between diagenesis, porosity reduction, and oil emplacement in late Carboniferous sandstone reservoirs, Bothamsall Oilfield*, E. Midlands, Geological Society of London Journal, **135**, 7-24.

Heald, M.T., (1955) *Stylolites in sandstones*, Journal of Geology, **63**, 101-114.

Heald, M.T., (1959) *Significance of stylolites in permeable sandstone*, Journal of Sedimentary Petrology, **29**, 251-253.

Heath, R., (1989) *Exploration in the Cooper Basin*, Australian Petroleum Exploration Association Journal, **29**, 366-378.

Houseknecht, D.W., (1988) *Intergranular pressure solution in four quartzose sandstones*, Journal of Sedimentary Petrology, **58**, 228-246.

Houseknecht, D.W., and Hathon, L.A., (1987) *Petrographic constraints on models of intergranular pressure solution in quartzose sandstones*, Applied Geochemistry, **2**, 507-521.

Hurst, A.R., (1980) *Occurrence of corroded authigenic kaolinite in a diagenetically modified sandstone*, Clays & Clay Minerals, **28**, 393-396.

Jourdan, A., Thomas, M., Brevart, O., Robson, P., Sommer, F., and Sullivan, M., (1987) *Diagenesis as the control of the Brent Sandstone reservoir properties in the Greater Alwyn area (East Shetland Basin*), in: Petroleum Geology of North West Europe: London, Graham and Trotmann Ltd., (eds. Brooks, J., and Glennie, K.), 951-961.

Laws, R.A., (1989) Preface. In: B.J. O'Neil (ed.), *The Cooper and Eromanga Basins, Australia*, Proceedings of the Cooper and Eromanga Basins Conference, Adelaide, 26-27 June 1989, v-vi.

Matter, A., and Ramseyer, K., (1985) *Cathodoluminescence microscopy as a tool for provenance studies of sandstones*,

in*:* Provenance of Arenites: Reidel, Dordrecht (Ed. Zuffa, G.G.), 191-211.

May, H.M., Helmke, P.A., & Jackson, M.L., (1979) *Gibbsite solubility and thermodynamic properties of hydroxy-aluminium ions in aqeous solution at 25^{o}C,* Geochimica et Cosmochimica Acta, **43**, 861-868.

McBride, E.F., (1989) *Quartz cement in sandstones: a review,* Earth-Science Reviews, 26, 69-112.

McCrea, J.M., (1950) *On the isotopic chemistry of carbonates and a palaeotemperature scale*, Journal of Chemical Physics., **18**, 849-857.

McLimans, R.K., (1987) *The application of fluid inclusions to migration of oil and diagenesis in petroleum reservoirs,* Applied Geochemistry, **2**, 585-603.

Morad, S., and Aldahan A.A., (1987) *Diagenetic replacement of feldspars by quartz in sandstones,* Journal of Sedimentary Petrology, **57**, 488-493.

Mozley, P.S., and Carothers, W.W., (1992) *Elemental and isotopic composition of siderite in the Kuparuk Formation, Alaska: effect of microbial activity and water/sediment interaction on early pore-water chemistry,* Journal of Sedimentary Petrology, **62**, 681-692.

Oelkers, E.H., Bjørkum, P.A., and Murphy, W.M., (1996) *A petrographic and computational investigation of quartz cementation and porosity reduction in North Sea sandstones,* American Journal of Science, **296**, 420-452.

Osborne, M., and Haszeldine, R.S., (1993) *Evidence for resetting of fluid inclusion temperatures from quartz cements in oilfields,* Marine and Petroleum Geology, **10**, 271-278.

Perny, B., Eberhardt, P., Ramseyer, K., Mullis, J., and Pankrath, R., (1992) *Microdistribution of Al, Li, and Na in a quartz: Possible causes and correlation with short-lived cathodoluminescence,* American Mineralogist, **77**, 534-544.

Pittman, E.D., (1979) *Porosity, diagenesis and productive capability of sandstone reservoirs,* in*:* Aspects of diagenesis (eds. Scholle, P.A., and Schluger, P.R.), *SEPM Special Publication* **26**, 159-173.

Porter, E.W., and James, W.C., (1986) *Influence of pressure, salinity, temperature and grain size on silica diagenesis in quartzose sandstones,* Chemical Geology, **52**, 259-369.

Prezbindowski, D.R., and Tapp, J.B., (1991) *Dynamics of fluid inclusion alteration in sedimentary rocks: a reveiw and discussion,* Organic Geochemistry, **17**, 131-142.

Prezbindowski, DR., and Larese, R.E., (1987) *Experimental stretching of fluid inclusions in calcite - Implications for diagenetic studies,* Geology, **15**, 333-336.

Ramseyer, K., and Mullis, J., (1990) *Factors influencing short-lived blue cathodoluminescence of* ?à*quartz,* American Mineralogist, **75**, 791-800.

Reynolds, T.J., (1978) *Fluid inclusion adapted U.S.G.S. gas flow heating/freezing instruction manual,* Fluid Incorporated, Denver.

Rezaee, M.R., (1996) *Reservoir Characterization of the Tirrawarra Sandstone, in the Moorari and Fly lake Fields, Cooper Basin, South Australia,* University of Adelaide, (unpublished Ph.D. thesis) 189 pp.

Rezaee, M.R., and Lemon, N., (1996) *Influence of depositional environment on diagenesis and reservoir quality: Tirrawarra Sandstone reservoir, southern Cooper Basin, Australia, Journal of Petroleum Geology,* **19**, 369-391.

Rezaee, M.R., and Schulz-Rojahn, J.P., (1998) *Application of quantitative back-scattered electron image analysis in isotope interpretation of siderite cement: Tirrawarra Sandstone reservoir, Cooper Basin (Australia),* In: Carbonate Cementation in sandstones (ed. Morad, S.), *International Association of Sedimentologists Special Publication,* **26**, 461-481

Rezaee, M.R., and Tingate, P.R., (1996) *Precipitation*

temperatures and origin of quartz cement and its influence on the Tirrawarra Sandstone reservoir quality, southern Cooper Basin, South Australia, Geological Society Of Australia, Abstract No.41, p.362. 13th Australian Geological Convention, Canberra, February, 1996.

Rezaee, M.R., and Tingate, P.R., (1997) *Origin of the quartz cement, Tirrawarra Sandstone, Southern Cooper Basin, South Australia,* Journal of Sedimentary Research, **67**, 168-177.

Rezaee, M.R., Lemon, N., and Seggie, R., (1997) *Tectonic fingerprints in siderite cement, Tirrawarra Sandstone, southern Cooper Basin, South Australia,* Geological Magazine, **134**, 99-112.

Roeder, E., (1984) *Fluid inclusions. Mineralogical society of America,* Reviews in Mineralogy 12, Washington.

Rosenbaum, J., and Sheppard, S.M.F., (1986) *An isotopic study of siderites, dolomites and ankerites at high temperatures,* Geochimica et Cosmochimica Acta, **50**, 1147-1150.

Schulz-Rojahn, J.P., (1991) *Origin, evolution and controls of Permian reservoir sandstones in the southern Cooper Basin, South Australia,* Unpublished Ph.D. thesis, National Centre for Petroleum Geology & Geophysics, University of Adelaide, Australia. 187p.

Sibley, D.F., and Blatt, H., (1976) *Intergranular pressure solution and cementation of the Tuscarora orthoquartzite,* Journal of Sedimentary Petrology, **46**, 881-896.

Siever, R., (1957) *Pennsylvanian sandstones of the Eastern Interior Coal Basin,* Journal of Sedimentary Petrology, **27**, 227-250.

Sommer, F., (1978) *Diagenesis of Jurassic sandstones in the Viking Graben,* Journal of Geologcal Society of London, **135**, 63-67.

Sprunt, E.S., (1981) *Causes of quartz luminescence colors,* Scanning Electron Microscopy, **1**, 525-535.

Stephan, H.J., (1970) *Diagenesis of the Middle Bunt sandstein in South Oldenburg, Lower Saxony*, Meyniana, **20**, 39-82.

Thomson, A., (1959) *Pressure solution and porosity*. In: Silica in sediments (ed. H.A., Ireland), SEPM Special Publication, **7**, 92-111.

Tupper, N.P., and Burckhardt, D.M., (1990) *Use of the methylphenanthrene index to characterise expulsion of Cooper and Eromanga Basin oils,* Australian Petroleum Exploration Association Journal, **30**, 373-385.

Walderhaug, O., (1990) *A fluid inclusion study of quartz-cemented sandstones from offshore mid-Norway - possible evidence for continued quartz cementation during oil emplacement,* Journal of Sedimentary Petrology, **60**, 203-210.

Walderhaug, O., (1994) *Temperatures of quartz cementation in Jurassic sandstones from the Norwegian continental shelf - evidence from fluid inclusions,* Journal of Sedimentary Research, **A64**, 311-323.

Waldschmidt, W.A., (1941) *Cementing materials in sandstones and their influence on the migration of oil,* AAPG Bulletin, **25**, 1839-1879.

Walker, T.R., (1960) *Carbonate replacement of detrital crystalline silicate minerals as a source of authigenic silica in sedimentary rocks,* AAPG Bulletin, **71**, 145-152.

Weyl, P.K., (1959) *Pressure solution and the force of crystallisation - A phenomenological theory*, Journal of Geophysical Research, **64**, 2001-2005.

Williams, B.P.J., and Wild, E.K., (1985) *Late Carboniferous-Early Permian sandstone reservoir facies analysis in hydrocarbon exploration of the Gidgealpa Group, Southern Cooper Basin, Southern Australia,* Abstract-Geological society of Australia, **12**, 553.